Critical behaviour of fully frustrated Potts models

2001 J. Phys. A: Math. Gen. 34 5183

(http://iopscience.iop.org/0305-4470/34/25/303)

INSTITUTE OF PHYSICS PUBLISHING JOURNAL OF PHYSICS A: MATHEMATICAL AND GENERAL

J. Phys. A: Math. Gen. **34** (2001) 5183–5200 PII: S0305-4470(01)21154-8

Critical behaviour of fully frustrated Potts models

D P Foster, C Gérard and I Puha

Laboratoire de Physique Théorique et Modélisation (CNRS ESA 8089), Université de Cergy-Pontoise, 5 Mail Gay-Lussac 95035 Cergy-Pontoise Cedex, France

Received 17 January 2001, in final form 6 February 2001
Published 15 June 2001
Online at stacks.iop.org/JPhysA/34/5183

Abstract

A numerical transfer matrix calculation is presented for two fully frustrated three-state Potts models on the square lattice: the Potts piled-up-domino model and the Potts zig-zag model. The ground state entropies and phase diagrams are found. The Potts piled-up-domino model displays a finite-temperature transition when the frustration effects are maximal, and displays re-entrant behaviour, in contrast to the Ising model equivalent. The ground-state entropy per spin is larger than in the Ising equivalent. The Potts zig-zag model displays the same qualitative behaviour as its Ising counterpart, and the ground-state entropy per spin is the same in the Potts and Ising cases.

PACS numbers: 0550, 0520, 6460F, 7510H

1. Introduction

Spin models are said to be frustrated when they contain competing interactions which prevent the simultaneous minimization of all the lattice bonds in the ground state [1]. The system is additionally described as fully frustrated if each plaquette of the lattice is itself frustrated [2]. The nature of a phase transition depends partly on the symmetry group of the candidate low-temperature phases. Frustration effects are then of most interest when they lead to infinitely degenerate or 'nearly degenerate' ground states. These will in general satisfy a larger symmetry group than the individual spins, possibly giving rise to exotic critical phenomena [3]. One such phenomenon is re-entrance [4]. This occurs when a disordered paramagnetic phase comes to lie at a lower temperature than an ordered phase; as the temperature is increased there is a transition from disorder to order. One possible explanation for this phenomenon is the so-called 'order by disorder' mechanism [5].

In this paper we present results for two fully frustrated three-state Potts models: the Potts piled-up-domino model (from here on referred to simply as the piled-up-domino model) and the Potts zig-zag model (or more concisely the zig-zag model). These are natural extensions of the Ising-model equivalents studied previously by André *et al* [6] and are defined as follows.

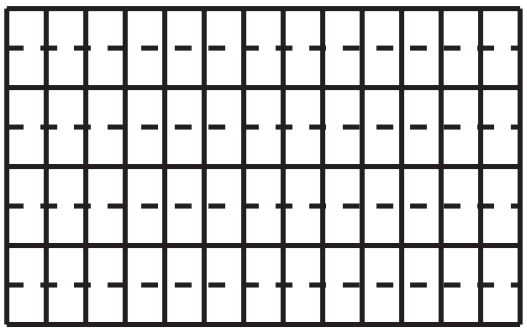

(*a*)

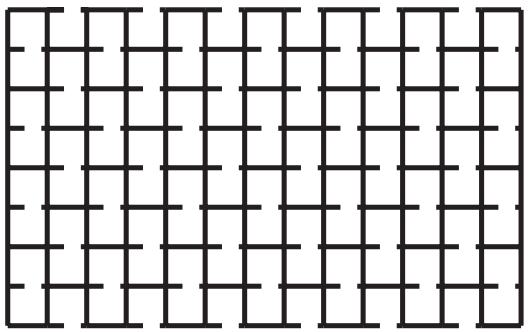

(*b*)

Figure 1. The piled-up-domino model (*a*) and the zig-zag model (*b*). The interaction energy is J_1 along the solid lines and J_2 along the dashed lines.

The q-state Potts model is defined as a set of variables $\{\sigma_i\}$ associated with the sites $\{i\}$ of a lattice [7]. Each σ_i takes one of q distinct values. The Hamiltonian of the model is given by

$$\mathcal{H} = -\tfrac{1}{2}\sum_{i,j} J_{i,j}\delta_{\sigma_i,\sigma_j} \tag{1}$$

where the sum runs over all pairs of sites and $J_{i,j}$ are the interaction strengths between a given pair of spins. For the models of interest in this paper, the interaction strengths are given by

$$J_{i,j} = \begin{cases} 0 & \text{for non-nearest-neighbour spins} \\ J_1 & \text{for nearest-neighbour spins along the solid lines} \\ J_2 & \text{for nearest-neighbour spins along the dashed lines} \end{cases} \tag{2}$$

as shown in figures 1(*a*) and (*b*) for the piled-up-domino and zig-zag models respectively. For convenience we define $\alpha = J_2/J_1$. J_1 will be taken as positive throughout. In this paper we shall concentrate on the $q = 3$ Potts models.

In the Ising versions of these models, the frustration effects suppress the critical temperature, which becomes zero when $\alpha = -1$ [8]. We show that, while this remains the case for the three-state Potts zig-zag model, the three-state Potts piled-up-domino model has a finite critical temperature when $\alpha = -1$ and displays re-entrant behaviour.

This paper is divided as follows: in the next section we present briefly the transfer matrix method used in our study, and in section 3 we apply this method to the calculation of the residual

ground-state entropy for the piled-up-domino model. We show that the residual ground-state entropy for the zig-zag model is exactly related to the equivalent Ising-model case. In section 4 we present the finite-temperature phase diagrams for the two cases and section 5 will be devoted to discussion.

2. The transfer matrix method

The results presented in this paper are obtained using a (numerical) transfer matrix calculation, giving the partition function for strips of finite width L but infinite length, $N \to \infty$. The results are therefore numerically exact for a given lattice width L.

The partition function for the model may be written in the form

$$\mathcal{Z} = \sum_{\{\sigma\}} \prod_{x} V(\mathcal{C}_x) H(\mathcal{C}_x; \mathcal{C}_{x+1}) \tag{3}$$

where $V(\mathcal{C}_x)$ is the contribution to the Boltzmann weight of a given column spin-state $\mathcal{C}_x$ due to interactions within a column and $H(\mathcal{C}_x; \mathcal{C}_{x+1})$ is the contribution due to interactions between adjacent columns, and depends on the spin states of the two columns $\mathcal{C}_x$ and $\mathcal{C}_{x+1}$. If additionally periodic boundary conditions are taken in the x-direction, the partition function for the system may be written as a trace over a product of transfer matrices:

$$\mathcal{Z} = \mathrm{Tr}\{\mathcal{T}^N\} \tag{4}$$

where $\mathcal{T} = V^{1/2} H V^{1/2}$ and the sum over spin states is taken care of by the matrix multiplications. Denoting the eigenvalues of $\mathcal{T}$ by λ_i,

$$\mathcal{Z} = \sum_i \lambda_i^N. \tag{5}$$

As N becomes large the partition function is dominated by the largest eigenvalue. The (dimensionless) free energy per spin, f is given by

$$\begin{aligned} f &= \lim_{N\to\infty} \frac{1}{NL} \log(\mathcal{Z}) \\ &= \frac{1}{L} \log(\lambda_0) \end{aligned} \tag{6}$$

and the correlation length is given by

$$\xi = \log\left(\frac{\lambda_0}{|\lambda_1|}\right) \tag{7}$$

where λ_0 is the largest eigenvalue and λ_1 is the second largest eigenvalue (in absolute value) [9].

The transfer matrix $\mathcal{T}$ is indexed by $\mathcal{C}_x$ and $\mathcal{C}_{x+1}$ both of which correspond to one of 3^L distinct column spin states. The capacity required to store the 3^{2L} matrix elements on a computer soon becomes prohibitive. In order to extend the range of values of L which may be treated numerically, the transfer matrix $\mathcal{T}$ is decomposed into a product of sparse matrices as follows.

One may view the transfer matrix as an operator which adds an additional column to the lattice. Each element of the matrix is indexed by the spin configuration on the last column of the lattice (L spins) and the spin configuration of the column being added. If we define a dangling bond as the bond which has only one spin attached to it, we see that the transfer matrix replaces the L existing dangling bonds with L new ones. The entry configurations and exit configurations are given by the values of the spins attached to these dangling bonds. If now, instead of adding a whole column at once, one spin is added at a time, there are still L dangling bonds beforehand and afterwards (see figure 2). This operation may be written as a

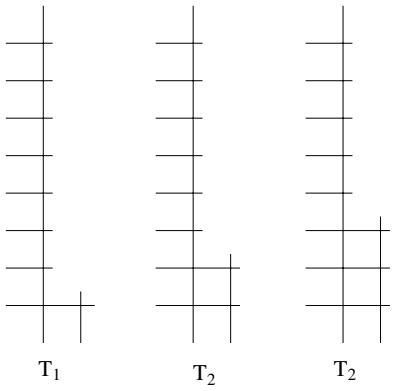

Figure 2. Construction of the transfer matrix by single spin addition.

matrix indexed by the configuration of the L spins connected to a dangling bond before the addition of the new spin, and the configuration of the L spins connected to a dangling bond after the spin addition. Since $L-1$ spins are common to the input and output configurations, the matrix elements will be non-zero only if these spins have the same values in the input and output configurations. The corresponding matrix is thus sparse. In this way $\mathcal{T}$ may be decomposed: $\mathcal{T} = \mathcal{T}_1\mathcal{T}_2^{L-2}\mathcal{T}_3$ where the matrices $\mathcal{T}_1$, $\mathcal{T}_2$, $\mathcal{T}_3$ correspond to one-spin additions. If the boundary conditions and in-column interactions are taken care of when the first and last spins are added, then the intermediary spin additions may all be performed by the same matrix. The combination of the $\mathcal{T}_i$ being sparse and the small number of distinct matrices required to build up $\mathcal{T}$ vastly reduces the storage requirements and enables calculation for lattice widths up to $L = 12$.

An alternative method for writing the transfer matrix involves the Kasteleyn–Fortuin mapping [10] to map the Potts model to a lattice animal problem [11]. This mapping requires periodic boundary conditions to enable a sparse-matrix reduction [11]. For $q = 3$ the transfer matrices in the two representations require an equivalent amount of storage but in a spin representation it is easier to implement the different boundary conditions used in this paper.

The eigenvalues used were calculated using the Lanczos method, using the ARPACK package.

3. Ground-state properties

In this section we calculate the ground-state entropy for the two models. In both models, when $\alpha > 0$ the model is ferromagnetic. While they are anisotropic, there is no competition in the interactions. The system minimizes its energy by choosing the same state for all the spins giving q distinct ground states [7, 12]. The entropy per spin is zero.

A lattice bond is 'satisfied' when the interaction energy along it is minimal, and 'frustrated' otherwise. It may be seen that for $\alpha < 0$ it is no longer possible to simultaneously satisfy all four bonds of a plaquette. The model is then said to be frustrated. However, if $\alpha > -1$ there is no ambiguity, in the ground state, over which bond to frustrate. The frustration does not change the ground state configuration, and the entropy per spin remains zero.

For $\alpha = -1$ the energy of a plaquette is minimal regardless of which bond is frustrated as long as one and only one bond is frustrated. There are an infinite number of frustrated bond configurations satisfying the ground state condition and the entropy per spin in this case is finite.

For $\alpha < -1$ the ground state degeneracy is still infinite. While it is clear that the system

Table 1. The ground-state entropy for the Potts piled-up-domino model. FBC: free boundary conditions. PBC: periodic boundary conditions.

L	$\alpha < -1$ FBC	$\alpha < -1$ PBC	$\alpha = -1$ FBC	$\alpha = -1$ PBC
2	0.502 5263	0.502 5263	0.635 098	0.635 0983
4	0.385 4409	0.358 8588	0.471 894	0.433 3004
6	0.352 1346	0.323 8563	0.430 075	0.393 4622
8	0.336 9267	0.311 3484	0.412 780	0.382 5248
10	0.328 266	0.305 7865	0.403 783	0.378 9744
12	0.322 6777	0.302 8948	0.398 421	0.377 6883
∞	0.299 9	0.297 2	0.381 4	0.376 6
Ising Exact	$\frac{1}{2}\log((1+\sqrt{5})/2)$ $= 0.240\,659\cdots$		$\frac{G}{\pi}$ $0.291\,6\cdots$	

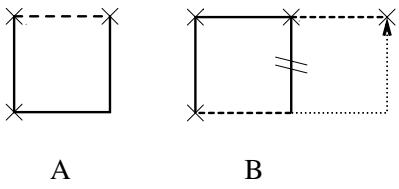

Figure 3. Plaquettes for the construction of the zig-zag model. Solid lines show interactions of strength J_1 and dashed lines interactions of strength J_2. The arrow shows path to prefixed spin in the case that the marked bond is frustrated.

will satisfy the antiferromagnetic bond in order to minimize the energy, there is still a choice over which of three ferromagnetic bonds to frustrate. The entropy per spin here is also finite.

3.1. Piled-up-domino model

The ground-state entropy for the piled-up-domino model was calculated using transfer matrices. In the ground state it is necessary to add two spins at a time in order to ensure that only one bond per plaquette is frustrated. Since the energy is constant and minimal, the entropy per spin is simply the number of ground states per spin, leading to

$$s = \frac{1}{L}\log(\lambda_0). \tag{8}$$

The entropy was calculated with the transfer direction parallel to the dashed lines as shown in figure 1. Both free and periodic boundary conditions were considered. The results are shown in table 1. It may be seen that the entropy per spin is substantially larger than for the Ising-piled-up-domino model.

The extrapolations to $L \to \infty$ throughout the paper are done using the Bulirch and Stoer algorithm [13].

3.2. The zig-zag model

The ground-state entropy per spin for the zig-zag model is the same in the Potts and Ising cases. This can be illustrated as follows: imagine that, from some suitable boundary configuration of spins, a ground-state configuration of spins is built up by adding alternately plaquettes of type A and B, shown in figure 3, in rows, starting from top left and ending bottom right, one plaquette at a time. The spins marked by a cross are shared with plaquettes already added to the lattice, and are thus already fixed. In the ground state only one bond per plaquette is frustrated. Whichever of the bonds is frustrated in a plaquette of type A, the 'free' spin is

connected by a ferromagnetic path to a predetermined spin. At first sight this is not true for plaquettes of type B, however the frustrated bond is shared between two plaquettes, and it can be seen that the 'free' spin is connected by a ferromagnetic path to a predetermined spin either directly, or via the neighbouring plaquette (of type A) see figure 3. The entropy per spin in the ground state is thus determined uniquely by the configurational entropy of the frustrated bonds, with no additional (local) degeneracy due to the number of Potts states. This was not so in the piled-up-domino case where it is possible to create free domains of spins. The residual ground-state entropy per spin is thus the same as reported for the Ising model [6], i.e.

$$s = \frac{1}{4\pi^2}\int_0^\pi \mathrm{d}\theta \int_0^\pi \mathrm{d}\phi \, \log\left[1 + 4\cos\theta\cos\phi + 4\cos^2\theta\right]$$
$$= 0.1615\cdots \qquad \text{for} \quad \alpha < -1$$
$$s = \frac{1}{4\pi^2}\int_0^\pi \mathrm{d}\theta \int_0^\pi \mathrm{d}\phi \, \log\left[4(\cos^2\theta + \sin^2\phi)\right]$$
$$= \frac{G}{\pi} = 0.2916\cdots \qquad \text{for} \quad \alpha = -1.$$

The difference between the ground states of the Ising and Potts versions of the zig-zag models is an overall degeneracy relating to the symmetry of the spin (Z_2 and Z_3). This was not the case for the piled-up-domino model, where the entropy per spin for the Potts case was significantly larger than the for Ising case for both $\alpha = -1$ and $\alpha < -1$. This difference indicates that the difference in symmetry group for the ground states in the two cases is not simply due to the difference in the symmetry groups of the spins. Based on these results, it is reasonable to expect that the phase diagram of the Potts zig-zag model should be qualitatively similar to the Ising case, but that the finite-temperature behaviour of the piled-up-domino model may well be qualitatively different. This is indeed what will be observed in the next section.

4. The finite-temperature phase diagrams

In this section we present the phase diagrams for the piled-up-domino and zig-zag models. The critical lines may be identified using phenomenological renormalization [14]. At a critical point the correlation lengths for two strip widths, measured as a fraction of the strip width, must be the same. This reflects the scale invariance of a critical system. In practice a finite width system is always off-critical; however,

$$\frac{\xi_L(T^*)}{L} = \frac{\xi_{L'}(T^*)}{L'} \tag{9}$$

gives a finite-size estimate of the critical temperature, T^*, which will tend to the true critical temperature as the strip widths tend to infinity. Assuming that the system is sufficiently close to the true critical point, the correlation length behaves (to leading order) as

$$\xi_L = A|T^* - Tc|^{-\nu}. \tag{10}$$

Since it is the finite width of the system which prevents the correlation length from diverging, at T^* we have $L \propto \xi_L$. If these two scaling laws are admitted, then a finite-size estimate of the correlation length exponent may be calculated from the equation

$$\frac{1}{\nu_{L,L'}} = \frac{\log\left(\frac{\mathrm{d}\xi_L}{\mathrm{d}T} \Big/ \frac{\mathrm{d}\xi_{L'}}{\mathrm{d}T}\right)}{\log\left(\frac{L}{L'}\right)} - 1. \tag{11}$$

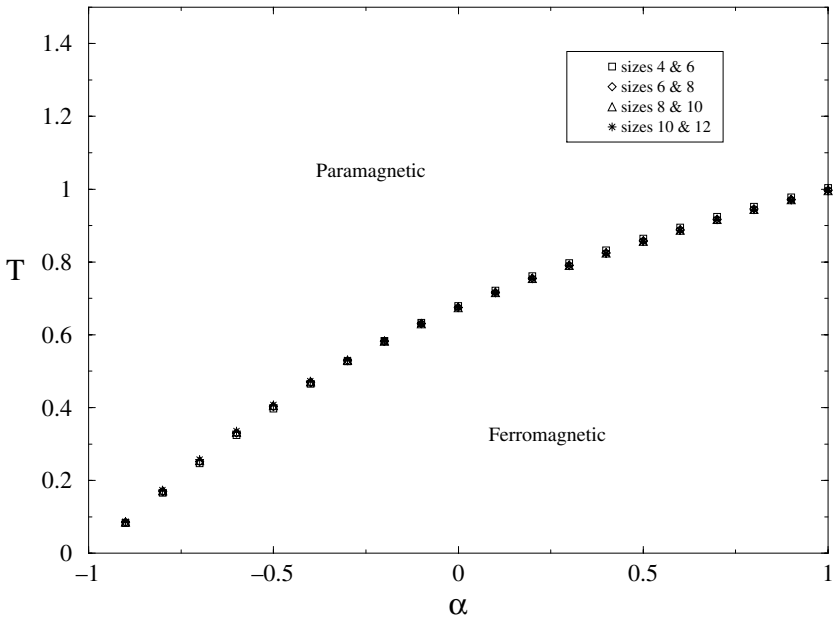

Figure 4. Phase diagram for the Potts zig-zag model.

Table 2. Critical temperature estimates for the zig-zag model.

L/L'	$\alpha = 1$	$\alpha = 0$
4/6	1.002 851 7	0.679 435 201
6/8	0.997 615 939	0.675 820 268
8/10	0.996 228 353	0.674 737 229
10/12	0.995 694 57	0.674 343 044
∞	0.995	0.674
Exact[a]	$1/\log(1+\sqrt{3})$ [15] $= 0.994\,973\cdots$	$= 0.673\,759\,6022\cdots$

[a] Critical temperature for $\alpha = 0$ solution of $e^{3/T} - 3e^{2/T} - 6e^{1/T} - 1 = 0$.

4.1. The zig-zag model

The phase diagram found using phenomenological renormalization for the zig-zag model with periodic boundary conditions is shown in figure 4. The finite-size effects are very small. The critical temperature is known exactly for two points on the phase diagram [12, 15]: $\alpha = 1$, corresponding to the pure ferromagnetic Potts model on the square lattice, and $\alpha = 0$, corresponding to the ferromagnetic Potts model on the hexagonal lattice. Our numerical values calculated at these two points are extrapolated and compared with the exact values in table 2.

Qualitatively the phase diagram is the same as for the Ising model: there is a phase transition between a low-temperature ferro-magnetic phase and a high-temperature phase for $\alpha > -1$. The critical temperature becomes zero at $\alpha = -1$ and there is no evidence of a phase transition for $\alpha < -1$.

The finite size estimates for the exponent ν are shown in figure 5. For a pure three-state Potts model ($\alpha = 1$ corresponding to the square lattice, and $\alpha = 0$ corresponding to the hexagonal lattice), the value of $\nu = 5/6$ is known exactly [16]. For $\alpha \geqslant 0$ the estimates

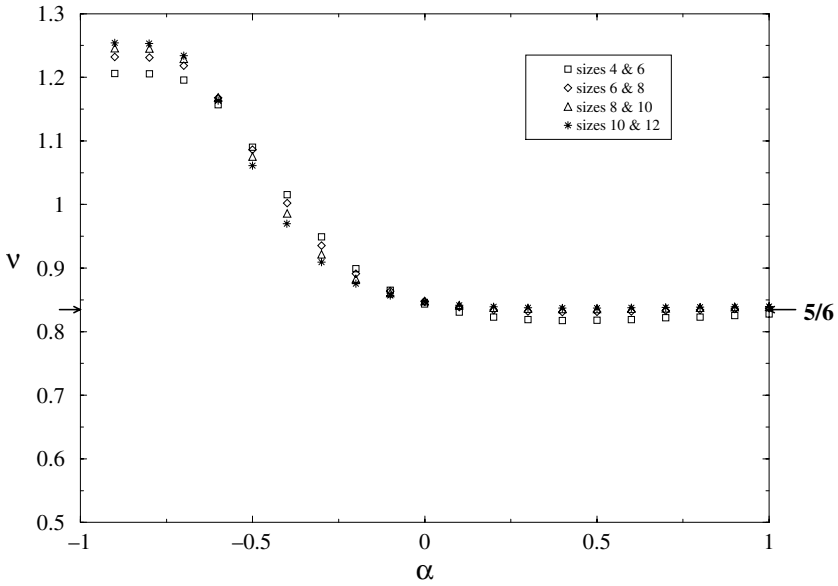

Figure 5. Finite size estimates for the exponent ν for the Potts zig-zag model.

for ν converge to the exact value. Close to $\alpha = -1$ the estimates for ν seem to take on a different value, but the range of values of α over which this variation is observed diminishes as the system size increases. There is no evidence of a multicritical point in the phase diagram between $\alpha = 1$ and -1, and so it would seem reasonable to assume that the whole line up to $\alpha = -1$ remains in the same universality class as the ferromagnetic three-state Potts model.

4.2. The piled-up-domino model

The phase diagrams for the piled-up-domino model with periodic and free boundary conditions found using phenomenological renormalization are shown in figure 6.

The critical temperature is known exactly for $\alpha = 1$ [12], the pure three-state Potts model on the square lattice, and at this point the critical temperature coincides trivially with that found in the zig-zag model. It may also be easily determined for $\alpha = 0$. When $\alpha = 0$ the spins on the dashed curves (see figure 1(a)) may be traced over. The resulting model is a ferromagnetic Potts model on a square lattice with different interactions in the x and y directions: $J_x = J_1$ and

$$\exp(\beta J_y) = \frac{\exp(2\beta J_1) + 2}{2\exp(\beta J_1) + 1}.$$

The critical temperature is known to satisfy [12]

$$(\exp(\beta J_x) - 1)\left(\exp\left(\beta J_y\right) - 1\right) = 3$$

which leads to $T_c = 1/\log(4)$, measured in units of J_1/k. In table 3 we compare the finite-size critical-temperature estimates, extrapolated using the Bulirch and Stoer algorithm [13], with the exact value calculated at $\alpha = 0$. The agreement is good.

Before trying to interpret the phase diagrams shown in figure 6 we review the main features of the Ising piled-up-domino model, reported in [6]. The phase diagram, shown in figure 7, is made up of two transition lines in the Ising model universality class. The transition

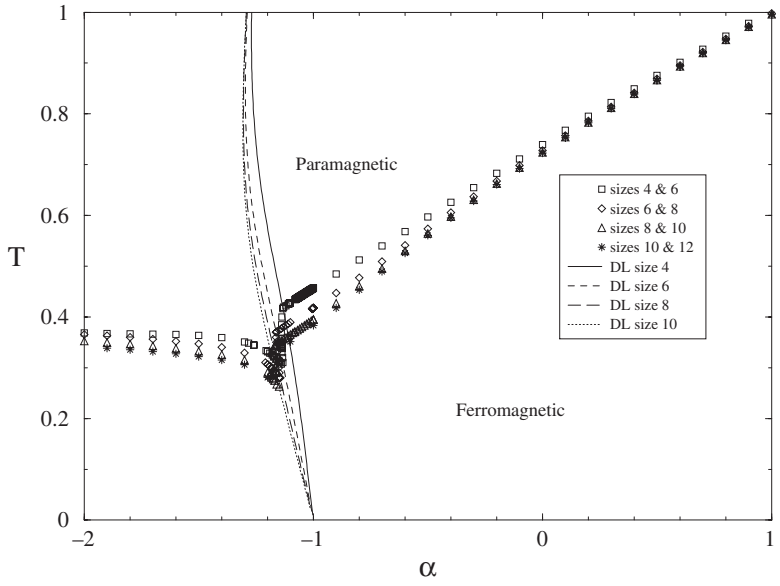

(*a*)

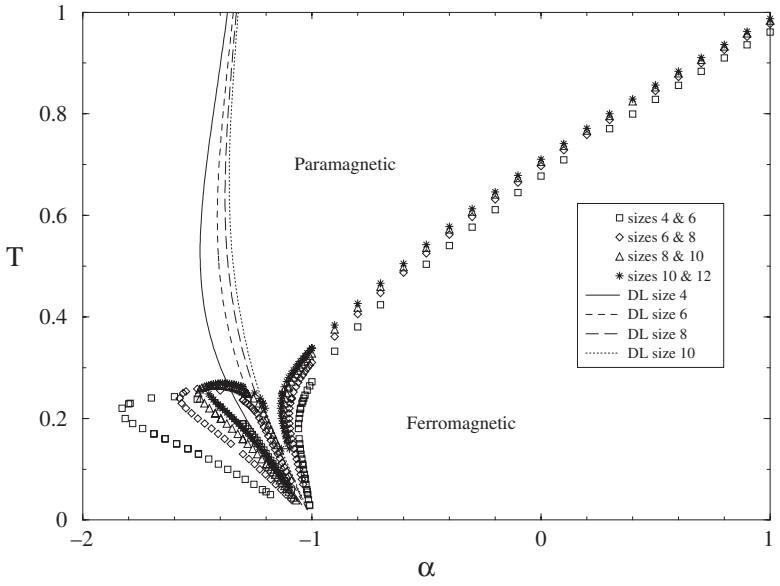

(*b*)

Figure 6. Phase diagram for the Potts piled-up-domino model with: (*a*) periodic boundary conditions and (*b*) free boundary conditions. The disorder lines are shown as curves, and the phase boundaries as symbols. The numerical uncertainty is smaller than the size of the symbols.

line for $\alpha > -1$ corresponds to the standard Ising transition between a ferromagnetic low-temperature phase and a paramagnetic high-temperature phase. For $\alpha < -1$ the ground state is highly degenerate. The low-temperature phase is characterized as follows: the spins on the

Table 3. Critical temperature estimates for the piled-up-domino model. PBC: periodic boundary conditions. FBC: free boundary conditions. PBC-y: periodic boundary conditions with the transfer direction perpendicular to the dashed curves (see figure 1).

	$\alpha = 0$		$\alpha = -1$			$\alpha = -1.3$	
L/L'	PBC	FBC	PBC	PBC-y	FBC	PBC	FBC
2/4	0.764 578	0.623 342	0.482 104	0.428 436	—	—	0.081 726
4/6	0.739 625	0.677 582	0.456 832	0.416 958	0.272 384	0.350 795	0.189 215
6/8	0.727 985	0.696 787	0.417 748	0.393 249	0.310 488	0.329 505	0.235 781
8/10	0.724 292	0.705 696	0.395 310	0.381 282	0.328 203	0.315 065	0.253 698
10/12	0.722 934	0.710 524	0.383 267	0.367 335	0.338 479	0.305 799	0.262 133
∞	0.722	0.722	0.361	0.367	0.379	0.283	0.274
Exact	$1/\log(4) = 0.721\,358\cdots$		—	—	—	—	—

antiferromagnetic lines order ferromagnetically in the y direction and antiferromagnetically in the x direction, where x and y directions are taken as in figure 1. The spins on the horizontal ferromagnetic lines are partially disordered. The transition is between this partially ordered antiferromagnetic phase and the high-temperature paramagnetic phase. The two transition lines meet with infinite slope at $\alpha = -1$, where the critical temperature is zero.

These results contrast with the phase diagrams shown in figure 6 for the three-state Potts models. The phase diagrams shown are calculated using finite width strips of width L in the direction perpendicular to the antiferromagnetic lines and infinite in the parallel direction. In figure 6(a) periodic boundary conditions are taken and in figure 6(b) free boundary conditions are taken. Periodic boundary conditions reduce the number of possible configurations available to the system, compared to the free boundary case, making it harder to excite the system, and tending to lock in the low-temperature phase. This is observed in the phase diagrams where in the periodic boundary case the critical temperature estimates converge to the thermodynamic limit from above, whilst for the open boundary case the critical temperature estimates converge from below (see also table 3). In table 3 we compare the critical-temperature estimates for the two boundary conditions for various key values of α and we find good agreement between the boundary conditions.

The two estimated phase diagrams are, however, quite different at first sight, notably for α less than about -1.3. Before trying to reconcile the differences, let us summarize the similarities. For $\alpha = -1$ there exists a finite-temperature phase transition with $T_c = 0.37 \pm 0.01$. In table 4 we show finite-size estimates for the exponent ν calculated using the two different boundary conditions. The extrapolated value of ν for the open boundary conditions at $\alpha = -1$ indicates a transition in the three-state Potts universality class. The finite-size estimates for $\alpha = -1$ with periodic boundary conditions are still too far from the thermodynamic limit to permit good extrapolation.

The point $\alpha = -1$ with $T = 0$ corresponds to a special point on the phase diagram, since it is the point which separates the ferromagnetic ground state ($s = 0$) from the frustrated highly degenerate ground state (s finite). It therefore corresponds to a transition point, which one would expect to be connected to the rest of the phase diagram. The phase diagram with open boundary conditions clearly shows a re-entrant phase ending in a multiphase point which we identify with the special point $T = 0$, $\alpha = -1$. Whilst the periodic boundary results do show the beginning of a re-entrant phase, the results are less clear. However, as we have seen, there is good agreement between the extrapolated critical temperatures right up to $\alpha = -1$. The transition lines become progressively more rounded as the system width increases. The failure

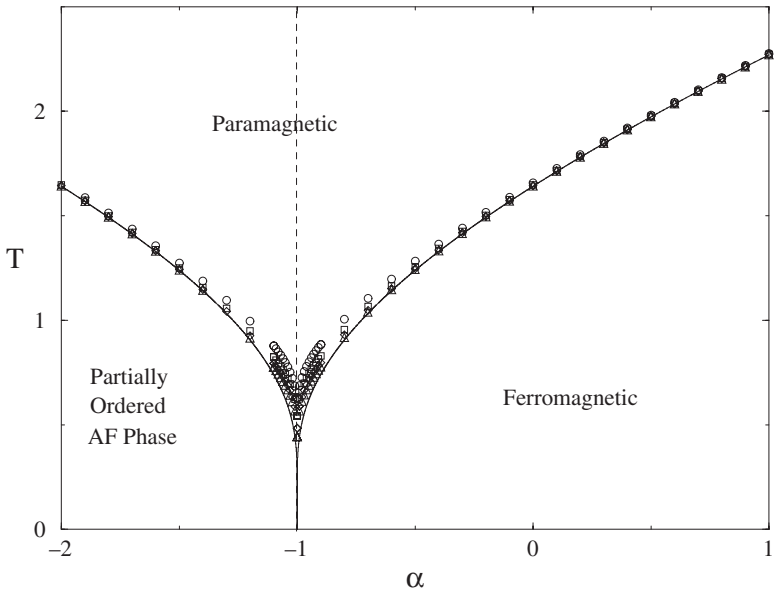

(*a*)

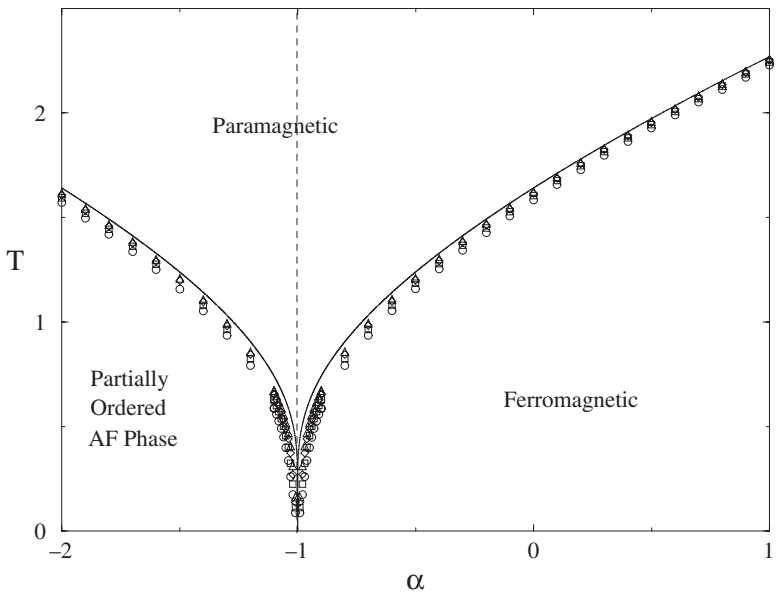

(*b*)

Figure 7. Exact phase diagram for the Ising piled-up-domino model, found by André *et al* [6] shown as solid curves along with the finite size estimates calculated from the phenomenological renormalization group for widths 6 and 8 (○), 8 and 10 (□), 10 and 12 (◇) and 12 and 14 (△). In (*a*) periodic boundary conditions are used, whilst in (*b*) open boundary conditions are used. The disorder line is shown as a dashed line and the phase boundaries as solid curves.

Table 4. Estimates for the exponent ν for the piled-up-domino model.

	Periodic boundary conditions			Free boundary conditions		
L/L'	$\alpha = 1$	$\alpha = 0$	$\alpha = -1$	$\alpha = 1$	$\alpha = 0$	$\alpha = -1$
2/4	0.807 155	0.727 115	0.457 417	0.897 734	0.770 501	—
4/6	0.827 697	0.754 573	0.505 535	0.891 758	0.836 442	2.049 413
6/8	0.837 053	0.792 602	0.573 436	0.883 714	0.852 665	1.354 167
8/10	0.839 283	0.811 782	0.639 087	0.877 283	0.857 856	1.162 991
10/12	0.840 722	0.821 423	0.697 795	0.872 277	0.859 395	1.075 589
∞	0.842	0.837	1.139	0.836	0.860	0.872

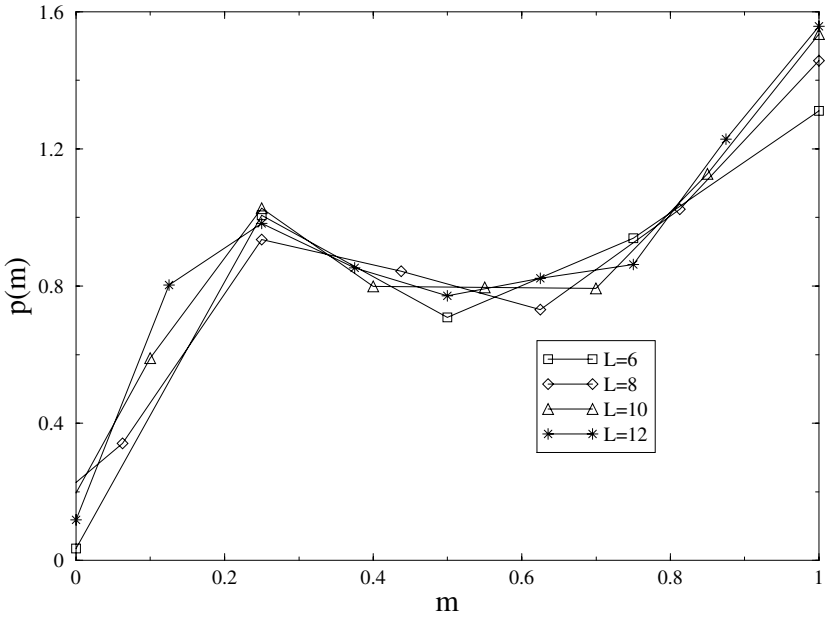

Figure 8. Probability density for the magnetization for $\alpha = -1.3$ and $T = 0.2$.

of the transition lines to reach $T = 0$ for the finite widths is probably related to a stabilisation of the low-temperature phase by the periodicity condition. To verify this conjecture, we compare the exact phase diagram found by André *et al* [6] with both periodic boundary condition and open boundary condition calculations, see figure 7. The convergence is excellent in both cases but, as for the Potts model, the periodic boundary condition results fail reach $T = 0$ (the transition lines for widths 12 and 14 reach $T = 0.444$), whereas the open boundary condition transition lines do extend right down to $T = 0$. In the light of these considerations it seems to us likely that the point $T = 0$, $\alpha = -1$ remains a multiphase point in the Potts model, where the paramagnetic, ferromagnetic and partially ordered phases meet. This view is confronted by the observation that the residual entropy per site at zero temperature is higher for $\alpha = -1$ than for either $\alpha < -1$ or $\alpha > -1$. This means that the ground state is more disordered at $\alpha = -1$ than for $\alpha < -1$ presumably due the coexistence of the paramagnetic and partially disordered phases.

In models with competing interactions, as is the case here, one may define disorder lines which indicate where the nature of the correlation function changes from monotonic (due to

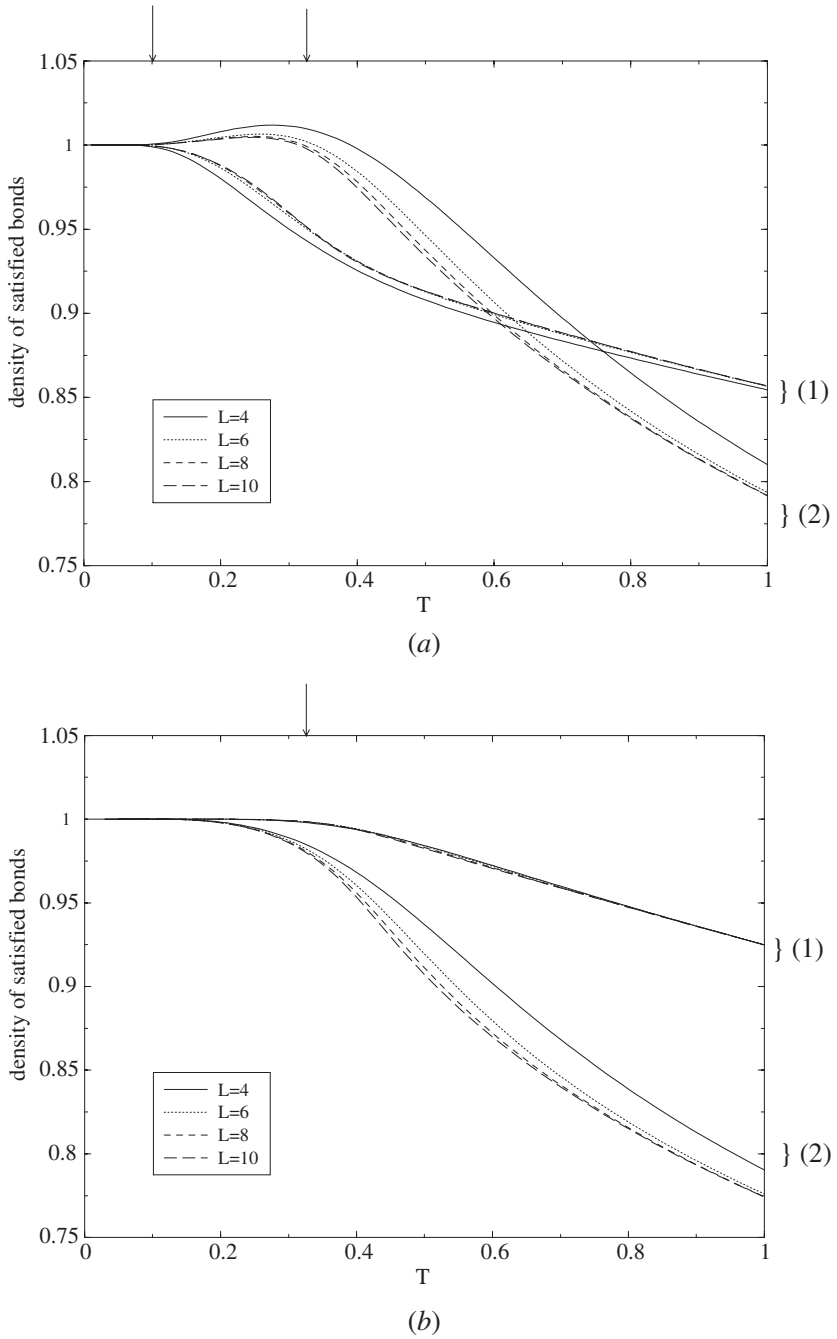

Figure 9. The set of lines in each graph labelled (1) shows the number of satisfied antiferromagnetic bonds normalized by the total number of antiferromagnetic bonds, while the set of lines labelled (2) shows the number of satisfied ferromagnetic bonds per spin. (*a*) Corresponds to $\alpha = -1.3$ and (*b*) to $\alpha = -2$ both with periodic boundary conditions.

the ferromagnetic interactions) to oscillatory (due to the antiferromagnetic interactions) [17]. It is easy to show that the correlation function (in the transfer direction) is related to the first and second largest eigenvalues in absolute value (the largest being always positive) through

$$G(x) \propto \left(\frac{\lambda_1}{\lambda_0}\right)^x. \tag{12}$$

If λ_1 is positive, then $G(x)$ is monotonically decreasing, but if λ_1 is negative then

$$G(x) = (-1)^x \left(\frac{|\lambda_1|}{\lambda_0}\right)^x$$

and is oscillatorily decreasing. If we define λ_1^+ as the largest positive eigenvalue, and λ_1^- as the largest (in absolute value) negative eigenvalue, then the disorder line is found when $\lambda_1^+ = |\lambda_1^-|$.

The disorder lines for various lattice widths are shown in figure 6 as lines. It is common to find disorder lines associated with re-entrant phases. In this case the disorder lines must enter the cusp caused by the re-entrant paramagnetic phase; since the disorder line corresponds to a change in behaviour of the correlation function it may not cross a critical line. The disorder lines for the two different boundary conditions may be seen to converge to a common line as the thermodynamic limit is approached. The limiting disorder line is curved, contrary to the Ising case, see the appendix, were the disorder line is calculated analytically and found to be a vertical line at $\alpha = -1$. The two transition lines join in the form of a cusp, with the disorder line between them (as in the Ising case). The form of the disorder line may then be seen as confirming the existence of the re-entrant paramagnetic phase.

Phenomenological renormalization indicates two possible phase diagrams depending on which boundary conditions were taken: either the transition line extends to $\alpha \to -\infty$ and the phase diagram resembles qualitatively a distorted version of the Ising model phase diagram, or there is a second re-entrance. The true thermodynamic phase diagram may correspond to one of the two possibilities discussed, or to a combination of the two, or indeed to neither.

In order to shed some light on this issue it is interesting to look at a variety of average thermodynamic quantities, such as the magnetization, energy, average numbers of each type of bond that are satisfied, etc. It is possible to calculate with relative ease such local average quantities in the framework of a transfer matrix calculation.

In order to calculate the magnetisation it is necessary to first calculate the probability of having configuration $\mathcal{C}_x$ in column x. This probability is simply the ratio of the partition function restricted to having configuration $\mathcal{C}_x$ and the unrestricted partition function, which in terms of transfer matrices may be written

$$p(\mathcal{C}_x) = \frac{\mathrm{Tr}\left\{T^x|\mathcal{C}_x\rangle\langle\mathcal{C}_x|T^{N-x}\right\}}{\mathrm{Tr}\left\{T^N\right\}}. \tag{13}$$

Writing $|\mathcal{C}_x\rangle$ in terms of the eigenvectors of T and taking N to infinity and using the fact the T is a real symmetric matrix leads to

$$p(\mathcal{C}_x) = \langle 0|\mathcal{C}_x\rangle^2. \tag{14}$$

The magnetization for the Potts model is defined as

$$m = \frac{1}{q-1}\left(q\langle n_{\max}\rangle - 1\right) \tag{15}$$

with $n_{\max}$ the maximum of $\{\rho_i\}$, where ρ_i are the densities of spins in each of the Potts states. Defining $m(\mathcal{C})$ as the magnetization for a column state as

$$m(\mathcal{C}) = \frac{1}{q-1}\left(q\frac{N_{\max}(\mathcal{C})}{L} - 1\right) \tag{16}$$

with $N_{\max}$ the largest of the numbers of each spin type present in configuration $\mathcal{C}$. The magnetization is then given as

$$m = \sum_{\mathcal{C}} m(\mathcal{C})\, p(\mathcal{C}) = \sum_{\mathcal{C}} m(\mathcal{C}) \langle 0|\mathcal{C}\rangle^2. \tag{17}$$

Since $\langle 0|\mathcal{C}\rangle^2$ is the probability of finding a column in configuration $\mathcal{C}$, then the probability of finding a column with magnetization m is given by

$$P(m) = \sum_{\mathcal{C}} \delta(m(\mathcal{C}) - m) \langle 0|\mathcal{C}\rangle^2. \tag{18}$$

It is important to note that this is *not* the probability of a magnetization m for the system as a whole. Since this probability distribution is restricted to a column it gives a finer probe into the probable column configurations. This is plotted for $\alpha = -1.3$ and $T = 0.2$ as a probability density function in figure 8 by dividing each probability by the interval between allowed values of the magnetization for a given lattice width. It may be clearly seen that the probability density is developing two peaks, one at $m = 1$ and a second at a substantially lower value of m. This implies that in the low-temperature phase each column has a high probability of being ordered ferromagnetically (along the y direction)or of being (partially) disordered. How these are arranged in the x direction is not easy to calculate in the transfer matrix formalism, but preliminary Monte Carlo calculations [18] seem to indicate that the system alternates in the x direction between ferromagnetically ordered and disordered columns. The probability distribution shown is virtually identical for the two considered boundary conditions and for $\alpha = -1.3$ and -2. The peak at $m = 1$ is lost in the high-temperature phase, clearly indicating the absence of magnetic order. No evidence of two different frustrated phases could be found from the distribution of the magnetization probability.

To calculate quantities such as the energy per spin or the densities of satisfied bonds it is necessary to calculate the probabilities of having a configuration $\mathcal{C}_x$ in column x and $\mathcal{C}_{x+1}$ in column $x + 1$ since these quantities are defined in terms of pairs of spins, which may belong to two adjacent columns. The calculation of the joint probability $p(\mathcal{C}_x, \mathcal{C}_{x+1})$ follows exactly as above:

$$p(\mathcal{C}_x, \mathcal{C}_{x+1}) = \frac{\operatorname{Tr}\left\{T^x |\mathcal{C}_x\rangle\langle\mathcal{C}_x| T |\mathcal{C}_{x+1}\rangle\langle\mathcal{C}_{x+1}| T^{N-x-1}\right\}}{\operatorname{Tr}\left\{T^N\right\}} \tag{19}$$

$$= \frac{\langle 0|\mathcal{C}_x\rangle\langle 0|\mathcal{C}_{x+1}\rangle\langle\mathcal{C}_x| T |\mathcal{C}_{x+1}\rangle}{\lambda_0}. \tag{20}$$

Defining $n_{\text{ferro}}(\mathcal{C}_x, \mathcal{C}_{x+1})$ and $n_{\text{antiferro}}(\mathcal{C}_x, \mathcal{C}_{x+1})$ as the densities of satisfied bonds, we may calculate the average values:

$$\langle n_{\text{ferro}}\rangle = \sum_{\mathcal{C}_x, \mathcal{C}_{x+1}} n_{\text{ferro}}(\mathcal{C}_x, \mathcal{C}_{x+1})\, p(\mathcal{C}_x, \mathcal{C}_{x+1}) \tag{21}$$

and similarly for $\langle n_{\text{antiferro}}\rangle$.

These two quantities are plotted in figure 9 for (*a*) $\alpha = -1.3$ and (*b*) $\alpha = -2$ with periodic boundary conditions. It may be seen that there is a clear difference of behaviour between $\alpha = -1.3$ and -2. In the first case the two densities may be seen to drop away from their maximal values at the different temperatures (shown approximately by arrows in figure 9(*a*)). In the second case this same drop off occurs at the same temperature for the two different densities. The results for the densities show a high degree of agreement between the two different boundary conditions. Both show a qualitative difference of behaviour between

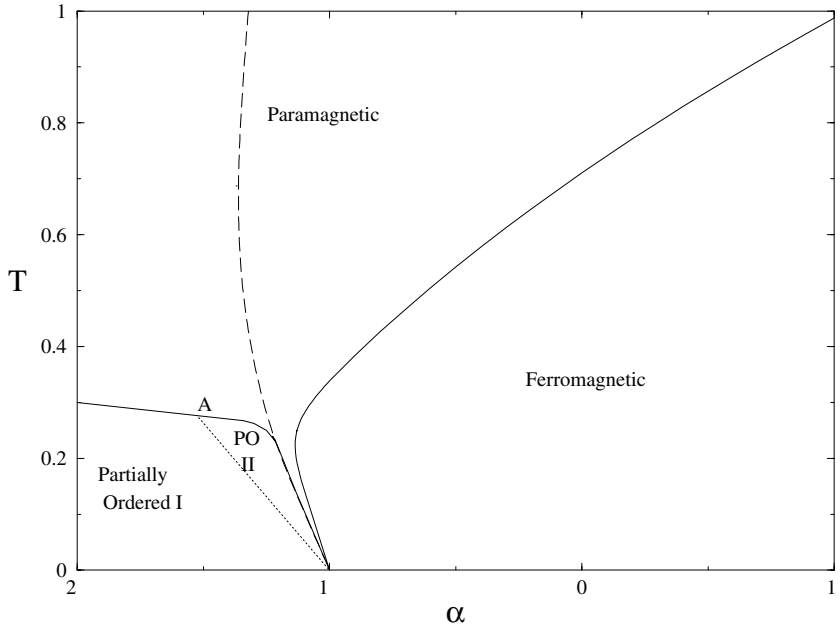

Figure 10. Possible thermodynamic phase diagram for the three-state Potts piled-up-domino model. The disorder line is shown as a dashed curve, and the dotted curve is a possible extra transition line between two partially ordered phases (see text) with a possible multicritical point, marked as A on the phase diagram.

$\alpha = -1.3$ and -2, and evidence of possible phase transitions for both values of α, indicated by arrows in figure 9, two for $\alpha = -1.3$ and one for $\alpha = -2$. The specific heat does not diverge with system size for either of these values of α, but the peaks of the specific heat converge to a temperature consistent with the critical temperature shown in figure 6(a) for α less than about -1.5 and all $\alpha \geqslant -1$.

We conclude that there is sufficient evidence to conjecture a phase diagram as shown semi-schematically in figure 10, with a possible second partially ordered phase at low temperature, (PO II). This additional phase, compared to the piled-up-domino Ising model, is only presented speculatively; the width of this phase reduces as system size increases (see figure 6) and may disappear in the thermodynamic limit. If such a phase were to exist then it is likely to terminate at a multicritical point (A). The presence of such a multicritical point could provide evidence of such a phase.

5. Conclusions

The main results presented in this paper relate to the Potts piled-up-domino model, where we have presented behaviour which is remarkably different from the equivalent Ising case, notably a finite-temperature transition and re-entrant behaviour. It is unusual to see re-entrance in such a simple model. Models showing re-entrance normally contain competing nearest-neighbour and next-nearest-neighbour interactions [3] or interaction between different spin types [19]. The additional entropy available due to the greater number of spin states stabilizes the ferromagnetic ground state as the temperature is increased (with $\alpha = -1$), contrary to the naive anticipation that the extra degrees of freedom will disorder the system more. This may be understood as

follows: in the Ising case the ground states may be mapped one to one onto dimer coverings of the lattice, but when the q-state Potts model is considered the mapping is no longer one to one, and the additional degeneracy is not uniformly distributed. This reweighting must apply to all the low-lying states, and must serve to stabilise the ferromagnetic phase as the temperature is increased through an order by disorder mechanism. In the zig-zag case the different dimer coverings have the same weight in the ground state, as in the Ising case, and we do not observe an equivalent stabilization of the ferromagnetic ground state.

The exact nature of the phase diagram and the low-temperature phases for $\alpha < -1$ remain to be fully determined, and will doubtless require other methods. This will be the object of a future study.

Acknowledgments

We would like to thank H T Diep, C Pinettes and T T Truong for interesting and useful discussions.

Appendix. Disorder line for the Ising piled-up-domino model

The free energy and phase diagram for the Ising piled-up-domino model was solved exactly by André *et al* [6], but to the best of our knowledge the disorder line has not been found for this model.

André *et al* give the (dimensionless) free energy per spin as

$$f = \log 2 + \frac{1}{4\pi^2}\int_0^\pi \int_0^\pi \mathrm{d}q_x\,\mathrm{d}q_y\,\log\Delta(q_x, q_y) \tag{A.1}$$

with

$$\begin{aligned}\Delta(q_x, q_y) = \tfrac{1}{2}[&\cosh 2\beta J\cosh 2\alpha\beta J + \cosh^2 2\beta J\cosh 2(1+\alpha)\beta J\\ &- \sinh^2 2\beta J\cos q_y - 2\cosh 2\beta J\sinh 2(1+\alpha)\beta J\cos q_x\\ &+ \sinh 2\beta J\sinh 2\beta\alpha J\cos 2q_x]\end{aligned} \tag{A.2}$$

from which we deduce the form of the generic correlation function as

$$G(q_x, q_y) = \frac{1}{\Delta(q_x, q_y)} \tag{A.3}$$

leading to

$$G(x, y) = \frac{1}{4\pi^2}\int_0^\pi \int_0^\pi \mathrm{d}q_x\,\mathrm{d}q_y\,\frac{\exp \mathrm{i}(xq_x + yq_y)}{\Delta(q_x, q_y)}. \tag{A.4}$$

The modulation of $G(x, y)$ in the x (y) direction is governed by the maximum of $G(q_x, q_y)$, or the minimum of $\Delta(q_x, q_y)$, with respect to $q_x(q_y)$. Since the modulation is anticipated in the x-direction (see [6]), we seek the turning points of $\Delta(q_x, q_y)$ with respect to q_x:

$$\frac{\partial\Delta}{\partial q_x} = 2\cosh 2\beta J\sinh 2(1+\alpha)\beta J\sin q_x - 2\sinh 2\beta J\sinh 2\alpha\beta J\sin 2q_x \tag{A.5}$$

which becomes zero when $q_x = 0,\ \pi$ or when

$$\cos q_x = \frac{\cosh 2\beta J\sinh 2(1+\alpha)\beta J}{2\sinh 2\beta J\sinh 2\alpha\beta J}. \tag{A.6}$$

Checking the second derivative of Δ it may be seen that the $q_x = 0$ solution is a minimum as long as

$$\cosh 2\beta J\sinh 2(1+\alpha)\beta J > 2\sinh 2\beta J\sinh 2\alpha\beta J \tag{A.7}$$

and the $q_x = \pi$ solution is a minimum as long as

$$\cosh 2\beta J \sinh 2(1+\alpha)\beta J > -2 \sinh 2\beta J \sinh 2\alpha\beta J. \tag{A.8}$$

These two conditions correspond exactly to the boundaries within which the solution (A.6) exists, which must correspond to a maximum.

In the range of values of α for which the two solutions $q_x = 0$ and π are minima it remains to determine which corresponds to the absolute minimum. This may be determined by considering

$$\Delta(\pi, q_y) - \Delta(0, q_y) = 4 \cosh 2\beta J \sinh 2(1+\alpha)\beta J. \tag{A.9}$$

This changes sign when $\alpha = -1$. For $\alpha > -1$ the leading mode of the correlation function is the $q_x = 0$ mode, while for $\alpha < -1$ the leading mode is the $q_x = \pi$ mode. This gives the location of the disorder line as $\alpha = -1$ for all temperatures.

References

[1] Toulouse G 1977 *Commun. Phys.* **2** 115
[2] Villain J 1985 *J. Physique* **46** 1840
[3] Diep H T (ed) 1994 *Magnetic Systems with Competing Interactions* (Singapore: World Scientific)
[4] Diep H T and Giacomini H 1994 *Magnetic Systems with Competing Interactions* (Singapore: World Scientific)
[5] Villain J, Bidaux R, Carton J-P and Conte R 1980 *J. Physique* **41** 1263
[6] André G, Bidaux R, Carton J-P and Conte R 1979 *J. Physique* **40** 479
[7] Potts R B 1952 *Proc. Camb. Phil. Soc.* **48** 106
[8] Villain J 1977 *J. Phys. C: Solid State Phys.* **10** 1717
[9] See for example: Yeomans J M 1992 *Statistical Mechanics of Phase Transitions* (Oxford: Oxford University Press) ch 5
[10] Kasteleyn P W and Fortuin C M 1969 *J. Phys. Soc. Japan* (suppl) **46** 11
[11] Blöte H W J and Nightingale M P 1982 *Physica* A **112** 405
[12] Wu F Y 1982 *Rev. Mod. Phys.* **54** 235
[13] Henkel M and Schütz 1988 *J. Phys. A: Math. Gen.* **21** 2617
[14] Nightingale M P 1976 *Physica* A **83** 561
[15] Baxter R G 1970 *J. Math. Phys.* **11** 784
[16] den Nijs M P M 1979 *J. Phys. A: Math. Gen.* **12** 1857
[17] Stephenson J 1969 *Can. J. Phys.* **47** 2621
Stephenson J 1970a *Can. J. Phys.* **48** 1724
Stephenson J 1970b *Can. J. Phys.* **48** 2118
Stephenson J 1970c *J. Math. Phys.* **11** 420
[18] Diep H T, Foster D P, Gerard C and Puha I 2001 *Preprint*
[19] Wood S M and Walker J S 1994 *J. Phys. A: Math. Gen.* **27** 3007